Design and test of the arc-shaped nail-tooth roller residual film recovery machine from the sowing layer

Zhiyuan Zhang[1,2,3†], Xuegeng Chen[1,2,3], Xianfei Wang[1,2,3†], Shuaikang Xue[1,2,3], Jingbin Li[1,2,3*]

(1. *College of Mechanical and Electrical Engineering, Shihezi University, Shihezi 832003, Xinjiang, China*;
2. *Xinjiang Production and Construction Corps Key Laboratory of Modern Agricultural Machinery, Shihezi 832003, Xinjiang, China*;
3. *Key Laboratory of Northwest Agricultural equipment, Ministry of Agriculture and Rural Affairs, Shihezi 832003, Xinjiang, China*)

Abstract: Residual films on the sowing layer produced after mulching in Xinjiang farmland, harm the sowing quality and root growth of crops. In this study, a sowing layer residual film recovery machine based on a radial plate arc-shaped nail-tooth roller structure was designed. Meanwhile, the key device structures were designed and the main working parameters were analyzed. Then, taking the working depth, the forward speed of the machine and the rotation speed of the nail tooth roller as the test factors, and the film collection rate and film intertwining rate as the test indicators, the single factor tests and the Box-Behnken response surface tests were carried out to evaluate the performance of the sowing layer residual film recovery machine. Consequently, the results showed that the order of significant factors was the working depth, the forward speed of the machine, and the rotation speed of the nail tooth roller. Besides, the optimal working parameters were determined, which the working depth, the forward speed of the machine, and the rotation speed of the nail tooth roller were 100 mm, 4.8 km/h, and 49.3 r/min, respectively. Moreover, the predicted value of the film collection rate was 69.20%. Finally, the verification test was taken with the optimal working parameter, and the results showed that the film collection rate was 66.84%, and the film intertwining rate was 1.39%. The relative error between the test value and the predicted value of the film collection rate was 3.40%. It indicated that the machine can perform the collection of sowing layer residual films. This study can provide a theoretical basis and reference for the design of new sowing layer residual film machines.
Keywords: residual film recycling machine, mulching film, pick-up device, seedbed preparation
DOI: 10.25165/j.ijabe.20241701.6993

1 Introduction

Film mulching is one of the most important agricultural means of production in China. It can warm the soil, preserve soil moisture, effectively improve the yields and quality of crops, and ensure national food security and the responsive supply of major agricultural products[1,2]. At present, both the amount of agricultural mulching film used and the area covered in China are the first in the world. However, the overuse of mulching films and insufficient concern for the collection have caused serious pollution problems of residual films in farmland and significantly affected the ecological environment of the sowing layer[3,4], sowing quality, root growth, and agricultural activities[5,6], restricting the agricultural green development of China[7-9].

An efficient and reliable residual film recovery machine is the key to solving mulching film pollution. In the past decades, researchers have conducted extensive research on the key

technology and equipment of farmland mulching film recovery. According to the different key film collecting parts, it can be divided into different types spring-tooth type, vibration-type, chain-tooth type, and roller-type[10,11]. Lu et al.[12-14] investigated the raking film tooth and film stripper of spring-tooth type film collector and obtained the optimal parameters combination of the model machine through field tests. However, this type of film collector presented a low collection rate of residual films in the plow layer. Ma et al.[15-17] studied the key operating components and operating parameters of the vibrating screen residual film recovery machine, and the results showed that this type of film collector has a high collection rate of film in the plow layer, but low working efficiency and high energy consumption. Sun et al.[18-20] analyzed the major film pick-up part of chain-tooth type film collector. Although the depth of such film collector would exceed 100 mm, it comes along with the side effects of forming heap soil or missing films during operation. Liu et al.[21-23] discussed the performance of roller-type film collectors and found that it could accomplish the residual films collection well, but there were problems with roller heaping soil and intertwining films. Hence, the farmland residual film recovery machine has been widely studied and developed, but there are still some problems with heaping soil, low efficiency, spike teeth intertwining with films, and so on.

Therefore, to improve the soil seedbed quality at the sowing layer, reduce the influence of residual films on seed germination and root growth. According to the distribution of residual films in Xinjiang farmland and combined with the findings of previous studies on plow layer residual film recovery machines, a sowing layer soil residual film collection method was proposed in this

study. Then, an arc-shaped nail-tooth roller-type sowing layer residual film recovery machine was designed based on the radial plate arc-shaped nail-tooth roller structure. Meanwhile, the structural and working parameters of the major parts were studied, and the best working parameters combination was determined based on the field test. This study can provide a theoretical basis and technical support for the development of new residual film recovery machines.

2 Structure and working principle of the residual film recovery machine

2.1 Structure and technical parameters

The arc-shaped nail-tooth roller-type sowing layer residual film recovery machine mainly consists of a traction unit, spring screw depth limiting device, rack, drive system, radial plate arc-shaped nail-tooth roller, film dripping unit, depth limiting wheel and film collection tank, etc. The traction unit is hinged with the rack by a hinge pin ear plate. The hydraulic depth limiting unit is fixed to the rack with a U-shaped bolt. The nail-tooth roller and film stripping unit are fixed to the rack with bolts. The structure of the whole residual film recovery machine is shown as Figure 1. The major technical parameters are listed as Table 1.
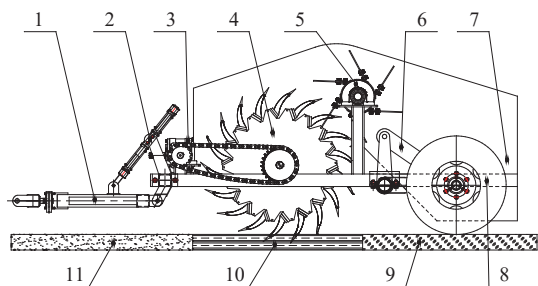
1. Traction unit 2. Spring screw depth limiting device 3. Drive system 4. Radial plate arc-shaped nail-tooth roller 5. Film dripping unit 6. Hydraulic depth limiting device 7. Film collection unit 8. Rack 9. Operated area 10. Operating area 11. Un-operated area

Figure 1   Structure of arc-shaped nail-tooth roller-type sowing layer residual film recovery machine

Table 1   Main technical parameters of the machine

Parameters	Values
Linkage method	Traction
Machine size (length×width×height)/m³	3.3×4.7×1.7
Mated power/kW	≥120
Working width/m	3.6
Working depth/mm	0-100
Working speed/km·h⁻¹	4-6
Working efficiency/hm²·h⁻¹	≥1.67
Machine weight/kg	4500

2.2 Working principle

The proposed residual film recovery machine is trailed by a tractor. The RPTO of the tractor provides power to the drive system of the device, and the drive system then distributes the power to the nail-tooth roller and the film stripping unit to pick and strip residual films successively. The operation process was: 1) the spring screw depth limiting device and the hydraulic depth limiting device adjust the operation depth of the operation machine; 2) the operation machine moves forward and the nail-tooth roller rotates in a clockwise direction; 3) the arc-shaped nail teeth stick into the soil and the residual films in the sowing layer; 4) the picked residual

films rotate with the roller until they get to the film stripping unit; 5) the films on the nail teeth are scraped by the flexible scraper on the counterclockwise rotating film stripping unit; 6) the scraped films are thrown into the film collection tank under the interactive effect of inertial forces and airflow field. During the operation, the spring screw depth limiting device has a certain buffering effect on the mutational force produced, thus preventing the working nail-tooth roller from instantaneous destruction when encountering hard objects such as rocks. The hydraulic depth limiting device can adjust the working depth of the machine and lift the distance between the major parts of the machine with the ground, facilitating the transportation of the machine.

3 Design of main parts and parameters

3.1 Design of arc-shaped nail tooth
3.1.1 Structural design of arc-shaped nail tooth

At present, the nail teeth or spring teeth are the key components of the residual film recovery machine, which is made of round steel with good plasticity and wear resistance. In operation, there are problems of difficulty in picking up and removing the film. Therefore, a kind of arc-shaped nail tooth with the shape of a triangular pyramid was designed in this study, it mainly consists of the tooth holder, tooth body, and tooth tip, as shown in Figure 2. The tooth holder is integrated with the tooth body by a screw thread pair so that worn tooth tips can be replaced easily. The tooth body is fixed with the tooth tip with a screw thread pair, too. Farmland residual films are mainly distributed in the 0-300 mm plow layer. Residual films with an area of 4-25 cm² take up 70% of the total residual films. The number of residual films in the 0-120 mm plow layer exceeds 60% of the total quantity, especially the larger films which are relatively stable in 0-50 mm topsoil[24,25]. On this basis, the arc-shaped nail teeth was used with the following parameters: total height L=200 mm, tooth body height L_1=140 mm, tooth tip height L_2=60 mm, tooth holder size $a×b$=60×100 mm².
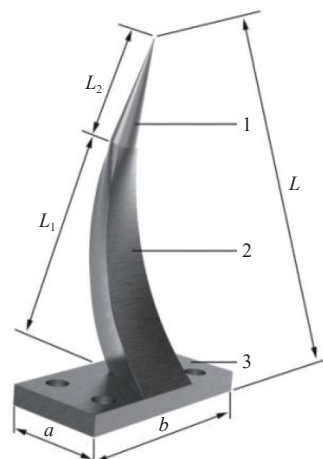
1. Tooth tip 2. Tooth body 3. Tooth holder

Note: L is the total height, mm; L_1 is the tooth body height; L_2 is the tooth tip height, mm.

Figure 2   Structure of arc-shaped nail tooth

3.1.2 Motion analysis and parameters determination of arc-shaped nail tooth

During field operation, the tooth tip and tooth body of arc-shaped nail tooth stick into the soil and the residual films, and pick out the films. According to the movement forms of the arc-shaped nail tooth in the soil, the tooth tip o was used as the origin to formulate a rectangular coordinate system o-xy, and the force

analysis was performed as Figure 3a. As shown, v is the machine forward speed, m/s; F is the tractive force, N; F_n is the sustaining strength of soil for the arc-shaped nail tooth, N; f is the resistance of soil to the nail tooth, N; m_g is the gravity of the nail tooth, N; β is the penetrating angle of the nail tooth, rad.

a. Force analysis   b. Bending angle analysis
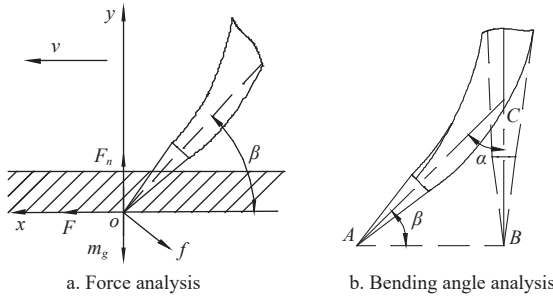
Figure 3   Theoretical analysis of the arc-shaped nail tooth

During operation, the friction acting on the film stripping part would reach maximum when the working part gets into the soil completely. At this time, the tractive force in the *ox* direction can be obtained according to the force equilibrium equation as follows:

$$F = f\sin\beta \qquad (1)$$

The resistance to the arc-shaped nail tooth in the soil is mainly caused by soil friction, soil deformation, and forward resistance. The soil resistance f can be obtained through the following soil resistance equation:

$$f = f_0 mg + Kab + \varepsilon abv^2 \qquad (2)$$

where, f_0 is the combined friction coefficient, usually f_0=0.3-0.5; K is a coefficient related to soil deformation and cutting resistance. Usually, the sandy soil or sandy loam uses K=2 N/cm², sandy clay uses K=4 N/cm², clay uses K=6 N/cm², and heavy clay uses K=6-10 N/cm². The soil in northern Xinjiang is mainly light and medium loam, while southern Xinjiang is mainly sandy and light-medium loam, so the coefficient was selected as K=2-4 N/cm²; ε is a coefficient related to the penetrating depth and actual working width, usually ε=4000 N·s²/m⁴; a is the penetrating depth, mm; b is the actual working width, mm.

The tractive force of the mated tractor is concerned with the actual working width of the arc-shaped nail tooth, that is

$$F = \frac{F_0 b}{\eta} \qquad (3)$$

where, F_0 is the coefficient of the resistance to the working width of the nail tooth, 80-210 N/m; η is the utilization coefficient, ranging from 0.85-0.95.

Combine the above equations, the penetrating angle of the arc-shaped nail tooth can be obtained as:

$$\beta = \arcsin\frac{F}{f} \qquad (4)$$

Substitute the above parameters into Equation (4), it will have β=24.58°-37.85°.

In Figure 3b, BC represents the penetrating state of the arc-shaped nail tooth before bending; AC represents the penetrating state of the nail tooth after bending. ΔABC is a right triangle, where β is the penetrating angle of the arc-shaped nail tooth, α=52.15°-65.42°. So the bending angle of the tooth body is ranged from 52.15°-65.42° and 60° was used in this study.

3.1.3 Strength examination of arc-shaped nail tooth

To avoid any damage to the arc-shaped nail tooth in the soil, a strength analysis was conducted with ANSYS finite element analysis software. The tooth body is made of nodular cast iron. The mass density is 7.20×10^3 kg/m³, the Poisson's ratio is 0.30, the elasticity modulus is 2.06×10^{11} N/m², and the yield strength is 560 MPa. The tooth tip is made of Q235 round steel. The mass density is 7.85×10^3 kg/m³, the Poisson's ratio is 0.274, the elasticity modulus is 2.10×10^{11} N/m², and the yield strength is 235 MPa. Based on the calculation of Section 2.1.2, the simulation test on arc-shaped nail tooth is performed under maximum load conditions. The simulation results are shown as Figure 4.
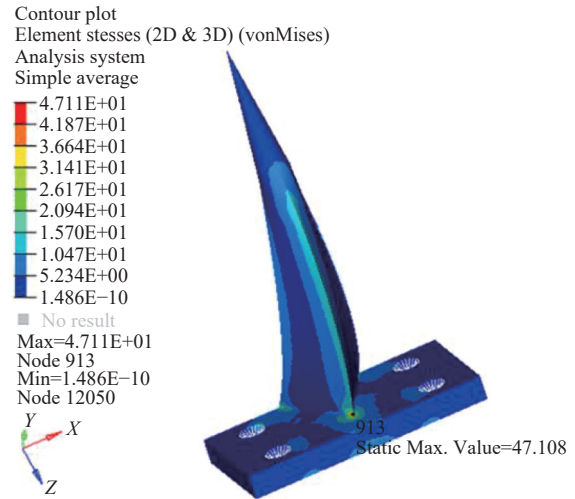
Figure 4   Stress nephogram of arc-shaped nail tooth

As shown in Figure 4, the maximum stress under the maximum load condition happened at the juncture between the tooth body and the tooth holder. The maximum stress is 47.11 MPa, much lower than the yield strength of the tooth body made of nodular cast iron, indicating that the arc-shaped nail tooth can satisfy the strength requirement.

3.2 Design of nail-tooth roller

3.2.1 Design of nail-tooth roller and arrangement of arc-shaped nail teeth

The nail-tooth roller is a major working part of the residual film recovery machine. The structure of the nail-tooth roller has effects on the working performance of the collector. Current full plate roller devices would produce excessive heap soil and consume a large amount of energy. To solve these problems, a radial plate nail-tooth roller device was designed in this paper, as shown in Figure 5a. The device mainly consists of the arc-shaped nail teeth, flange roller central shaft, radial plate, holder, etc. The main body of the device was produced by the welding technique. During the picking process, the nail-tooth roller can release the accumulated soil produced ahead through the gap between two holders, which can effectively solve the heap soil problem of the nail-tooth roller unit. According to the working width requirement, two nail-tooth roller units were installed side by side. For each roller, the effective working width is 1600 mm, the total length is 1900 mm, the maximum rotating diameter is 950 mm, and the distance between two radial plates is 236 mm. The holders were uniformly distributed in the peripheral direction of the nail-tooth roller unit. Each row of holders can accommodate 12-13 arc-shaped nail teeth. The distance between two adjacent teeth is 100 mm, and the arc-shaped nail teeth were fixed to the holders through four bolts (GB/T 5783-2016, hexagon head full-thread bolt M12×30). The distribution of residual films in soil has a variety of forms. The research showed that larger residual films behaved stable in 0-50 mm topsoil within 15 years after drip irrigation under mulch[26]. So, based on the distribution of nail teeth of the current full-plate roller device and the structural parameters

of arc-shaped nail teeth, an interlaced arrangement method was adopted in this paper. The distance between two circumferential

adjacent arc-shaped nail teeth is 50 mm. The expanded view of the arrangement method is shown as Figure 5b.
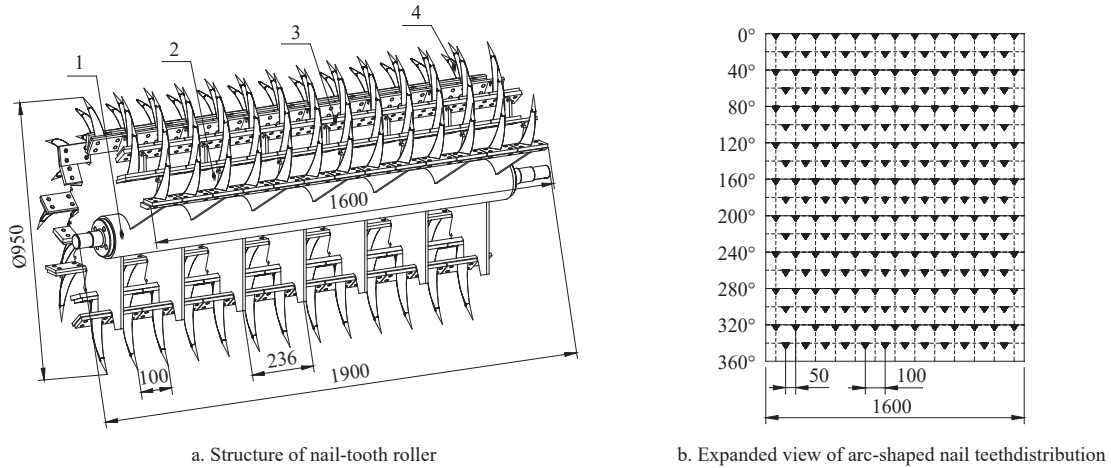
a. Structure of nail-tooth roller

b. Expanded view of arc-shaped nail teethdistribution

1. Flange roller central shaft 2. Radial plate 3. Holder 4. Arc-shaped nail tooth

Figure 5   Structure of nail-tooth roller and distribution of nail teeth (mm)

3.2.2　Motion analysis and parameter determination of nail-tooth roller

The nail-tooth roller makes compound movement during operation. The rotational velocity around the flange roller central shaft is relative, the forward velocity with the tractor is a transport velocity, so the movement trail of the arc-shaped nail tooth when the roller rotates is a trochoid, as shown in Figure 6a.

Figure 6 shows the movement trail of two circumferential adjacent arc-shaped nail teeth 1 and 2. AB refers to the period of the arc-shaped nail tooth penetrating the soil and residual film. BC refers to the nail tooth carrying and stripping the residual film. A rectangular coordinate system XOY was established by using the vertical line of tooth 2 passing the A_2 point as the y-axis, and the transverse line of the nail-tooth roller passing the lowest point as the x-axis. Then the trajectory equation of the nail tooth tip is:

$$\begin{cases} x = v_0 t + R\sin(\omega t) \\ y = R - R\cos(\omega t) \end{cases} \quad (5)$$

where, R is the maximum rotation radius of the nail-tooth roller, mm; ω is the angular velocity of rotation, rad/s; v_0 is the forward speed of the tractor, m/s; t is the movement time, s.

Make the first-order and second-order derivation on time t in Equation (5), the velocity and acceleration of the tooth tip can be obtained:

$$\begin{cases} v_x = v_0 + R\omega\cos(\omega t) \\ v_y = R\omega\sin(\omega t) \end{cases} \quad (6)$$

$$\begin{cases} a_x = -R\omega^2\sin(\omega t) \\ a_y = R\omega^2\cos(\omega t) \end{cases} \quad (7)$$

After calculation, the following equation can be obtained:

$$\begin{cases} v = \sqrt{v_0^2 + R^2\omega^2 + 2R\omega v_0\cos(\omega t)} \\ a = R\omega^2 \end{cases} \quad (8)$$

The circular velocity v of the rotating nail-tooth roller is larger than the forward velocity v_0 of the tractor, that is

$$\lambda = \frac{v}{v_0} \quad (9)$$

The working velocity of the machinery in this study was v_0=4-6 km/h. When λ=3-10, it will have ω=2.14-14.43 rad/s by combining Equations (8) and (9).

a. Movement trail of arc-shaped nail tooth

b. Analysis of continuous work
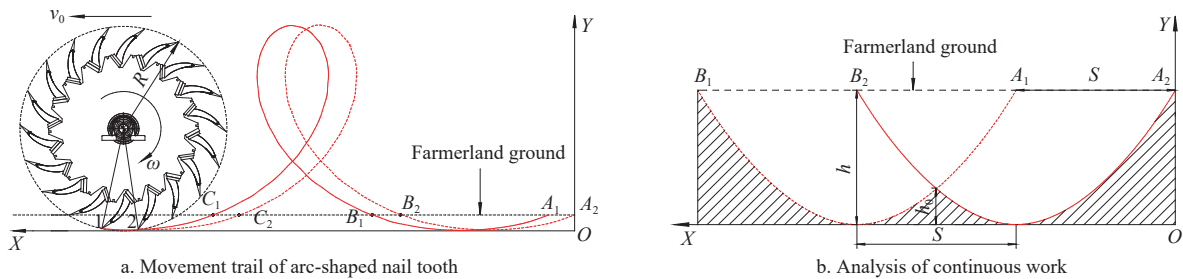
Figure 6   Motion analysis of nail-tooth roller unit

According to the relationship between the angular velocity and the velocity of circular movement, i.e. $\omega = 2\pi n$, the rotational speed of the nail-tooth roller can be obtained as n=20-137.80 r/min.

The collector should not only ensure the stable working depth but also accomplish the collection of all the residual films in the plow layer. To realize the working continuity of the device, a continuity analysis of two circumferential adjacent arc-shaped nail teeth is conducted as Figure 6b.

When the circumferential adjacent nail teeth successively penetrate the soil at time t, the distance of the device in the forward direction is the penetrating pitch S.

$$S = v_0 t \quad (10)$$

where, S is the penetrating pitch of the circumferential adjacent arc-shaped nail teeth, mm.

According to the structure of the nail-tooth roller, the interval

time of the successively penetrated circumferential adjacent arc-shaped nail teeth is,

$$t = \frac{2\pi}{z\omega} \tag{11}$$

where, z is the number of rows of installed circumferential arc-shaped nail teeth, row.

Combine Equations (9)-(11), the following equation can be obtained:

$$S = \frac{2\pi R}{z\lambda} \tag{12}$$

According to the area distribution of residual mulching films in Xinjiang cotton fields and the structural parameters of arc-shaped nail teeth, taking S=50 mm and being substituted into Equation (12), it will have z=5.9-19.8. To improve the collection efficiency and improve the penetrating times, take z=18.

When the circumferential adjacent arc-shaped nail teeth get through the films, there will be a protruding part in the soil. The protruding height h_0 is the distance from the joint of the trajectories of the arc-shaped nail teeth to the maximum penetration depth of the nail teeth. h_0 can be approximated as:

$$h_0 = R\left[1 - \cos\frac{\pi}{z(\lambda-1)}\right] \tag{13}$$

When the sowing depth of Xinjiang cotton is 25-35 mm, then:

$$h - h_0 > 35 \tag{14}$$

where, h is the maximum penetrating depth of arc-shaped nail tooth, mm. According to Equations (9) and (12)-(14), it will have h_{min}=43.75 mm.

3.3 Design of film stripping unit

The film stripping unit is a major part of the arc-shaped nail-tooth roller-type sowing layer residual film recovery machine. Its function is to separate the residual films on the arc-shaped nail teeth from the nail teeth and carry the residual films to the film collection tank. The film stripping unit mainly consists of a central shaft, blade bracing plate, blade pressing plate, film stripping blade, and bolts. The blade bracing plate is welded on the central shaft. The film stripping blade is fixed to the blade bracing plate through bolts and the blade pressing plate, as shown in Figure 7. According to the structural parameters of the nail-tooth roller unit, the total length of the film stripping unit was designed as 1885 mm, the effective working length is 1615 mm, and the maximum rotating diameter is 580 mm. An isosceles triangled notched film stripping blade was also used. The vertex angle of the isosceles triangle is 16°, and the length of the bottom edge is 45 mm. The film stripping blade was made of an 8 mm thick wear-resistant rubber plate, a total of 6 rows, each row with 25 notches.
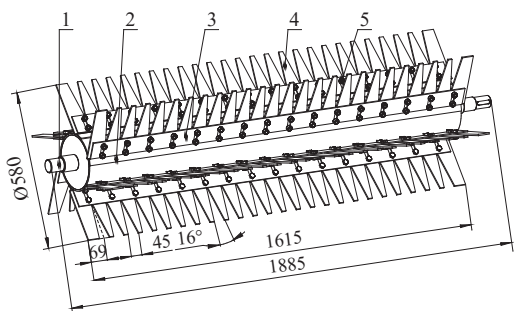
1. Central shaft 2. Blade bracing plate 3. Blade pressing plate 4. Film stripping blade 5. Bolts

Figure 7   Structure of the film stripping unit (mm)

3.4 Design of film collection and unloading unit

The film collection and unloading unit mainly consists of the rack, hydraulic cylinder, tank base plate, and film collection tank. The tank base plate was hinged with two side plates of the film collection tank through a hinge pin. The opening angle of the tank base plate was controlled by the expansion of the hydraulic cylinder, as shown in Figure 8. During operation, the residual films scraped by the film stripping blades are carried into the film collection tank under the common effect of the gravity and airflow produced by the film stripping unit. When the residual films in the tank reached a certain amount, the hydraulic cylinder would open the tank base plate and unload the films automatically, thus accomplishing the collection of residual films.
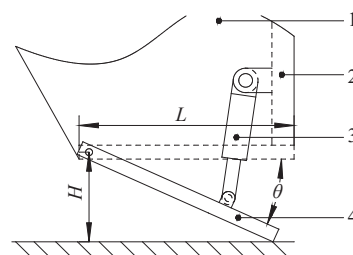
1. Film collection tank 2. Rack 3. Hydraulic cylinder 4. Tank base plate

Figure 8   Structure of film collection and unloading unit

To improve the working continuity and efficiency of the residual film recovery machine, reduce labor work and ensure the residual films in the collection tank slide smoothly from the tank base plate, the following relationship between the length L of the tank base plate and the height H of the film collection tank from the ground should be maintained, that is,

$$H > L\sin\theta \tag{15}$$

where, θ is the opening angle of the tank base plate, rad. This angle is associated with the sliding friction angle between the residual film and steel plate.

In the paper, the sliding friction angle between the residual film and steel plate was measured using the inclined plane method, as shown in Figure 9. During the tests, the residual film sample was put at the middle-upper part of the tiltmeter steel surface. To gradually increase the angle of the slope, the handle was turned slowly and evenly. Measured the slope angle δ when the sample continuously slides on the steel plate. This slope angle is the sliding friction angle between residual film and steel plate. Repeat the tests and average the results. The results showed that the sliding friction angle δ=23.30°. So the length of the tank base plate is determined as L=600 mm, and the height of the film collection tank from the ground is H=260 mm. Under this condition, the residual films can be automatically unloaded during the continuous working of the film collector.
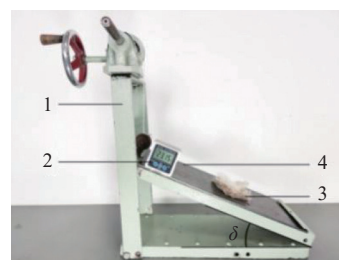
1. Tiltmeter 2. Digital angle gauge 3. Residual film 4. Steel plate

Figure 9   Sliding friction angle measurement

4   Field performance test and analysis

To test the operation performance of the arc-shaped nail-tooth roller-type sowing layer residual film recovery machine, and determine the optimal operation parameters. The field tests were conducted at Shihezi General Factory Farm 1 Company of the 8th Division of Xinjiang Production and Construction Corps, Shihezi, Xinjiang on May 7, 2021. The test process and effect are shown in Figure 10.

a. Field test process   b. Test effect
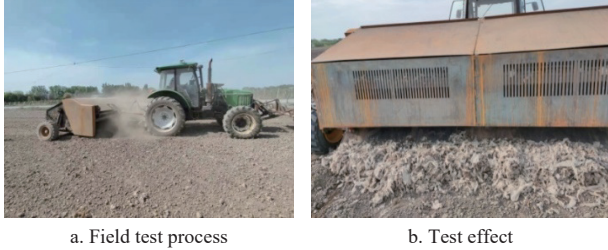
Figure 10   Field test of the residual film recovery machine

4.1   Test condition

The soil type in the test field is loam soil, and the tests show that the average soil firmness of 100 mm soil is 201 kPa, and the average moisture content is 23.1%. The test field was used to be cotton field with mulch films. It is of a good condition and land formation. The tillage depth is 200 mm, the loose soil rate is more than 80%, and the area of the test is about 1.33×10^4 m^2; the mated power for the machinery is provided by Tiantuo 1204 roller tractor. The rear output shaft velocity of the tractor is 540 r/min, and the forward speed is 4.0-6.0 km/h.

4.2   Test methods

The field performance tests of the prototype were performed according to the methods of GB/T 25412-2010 (Mulch Film Residue Collector). Five interlaced zones were selected randomly as the testing zones. The width of each testing zone is 10 m and the length is 100 m. In each testing zone, select five test points with equal spacing. Each test point is 1 m×1 m in size. The residual films (0-100 mm) were picked out before collection. Then select another five test points with equal spacing near the former five points (not overlapped with them) for after-collection points. Pick out the residual films from these five points after collection. Wash and dry the residual films collected, weigh and record the average weight. The residual film collection rate Y_1 was calculated according to Equation (16):

$$Y_1 = \frac{\sum\left(1 - \dfrac{m_0}{m}\right)}{5} \times 100\% \tag{16}$$

where, Y_1 is the collection rate of residual films, %; m_0 is the weight of films at the test points after the operation, g; m is the weight of films at the test points before the operation, g.

After field operation, the residual films in the film collection tank and those intertwined on the machine were taken out. The films were cleaned and dried and then weighed. Equation (17) was used to calculate the film intertwining rate Y_2:

$$Y_2 = \frac{\sum\left(\dfrac{m_1}{m_1 + m_2}\right)}{5} \times 100\% \tag{17}$$

where, Y_2 is the film intertwining rate, %; m_1 is the weight of residual films intertwining on the machine in the testing zone, g; m_2 is the weight of residual films in the film collection tank, g.

4.3   Test design

4.3.1   The single factor test design

To determine the value range of each working parameter of the arc-shaped nail-tooth roller plow layer residual film recovery machine, and obtain the influence rule of each working parameter on the operation index, a single-factor field performance test was conducted. According to References [23,26] and the theoretical calculation results, the working depth x_1, the forward speed of the machine x_2, and the rotation speed of the nail tooth roller x_3 were used as the testing factors, and the film collection rate Y_1 and film intertwining rate Y_2 were used as the testing indicators. The test results are shown as Figure 11.

a. Working depth   b. Forward speed of machinery   c. Rotation speed of nail-tooth roller
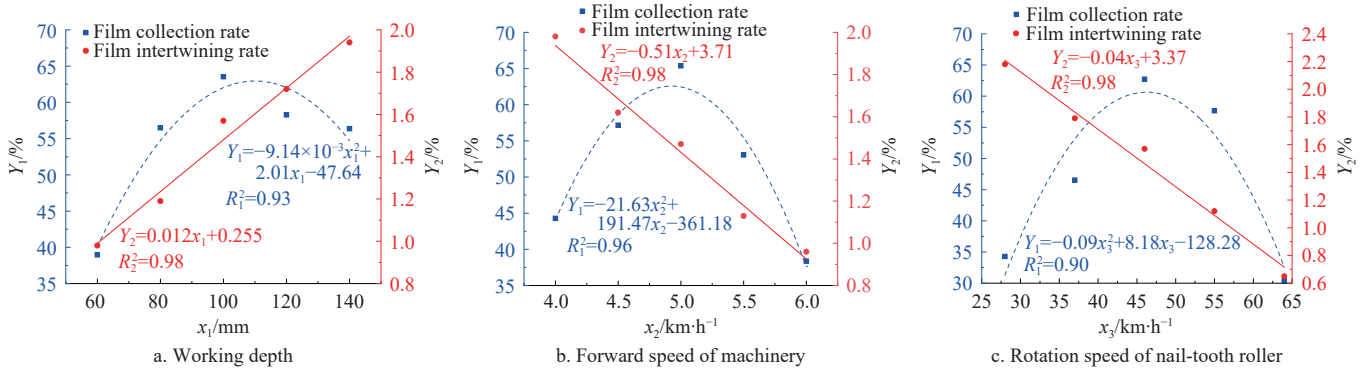
Figure 11   Influences of each factor on the residual film collection rate and intertwining rate

As shown in Figure 11, with the increase of the working depth x_1, the forward speed of the machine x_2, and the rotation speed of the nail tooth roller x_3, the film collection rate Y_1 increases first and then decreases, presenting a nonlinear change. The film intertwining rate Y_2 shows a linear variation relationship, and $Y_2 \leq 2\%$, which is in line with the value specified in national standard GB/T 25412-2010. Therefore, the research team of this study will carry out further research on the film collection rate Y_1.

In addition, according to Figure 11a, the device has the highest collection rate when working at 110 mm depth. But tests show that the soil content in residual films and power consumption of tractor would rise significantly when working deeper than 100 mm. Figure 11b shows that the device has a good performance when the device moves at the speed of 4.5 km/h. Figure 11c shows that the device has the best performance when the nail-tooth roller rotates at the speed of 46 r/min.

4.3.2   The response surface test design

According to the single factor test results, when the film collection rate $Y_1 > 40\%$, the parameter range of each factor was as follows: the working depth $x_1 \in [60, 140]$, the forward speed of the

machine $x_2 \in [4, 6]$, the rotation speed of the nail tooth roller $x_3 \in$ [35, 65]. On this basis, the Design-Expert V8.0.6.1 software was used to design a three-factor and three-level Box-Behnken center combination test to explore the influence of each factor and its interaction on the film collection rate Y_1. The test factors and level codes are listed in Table 2.

Table 2   Horizontal coding table of test factors

Levels	Factors		
	x_1/mm	x_2/km·h^{-1}	x_3/r·min^{-1}
Upper level(1)	140	6	65
Zero level(0)	100	5	50
Lower level(−1)	60	4	35

4.4   Results analysis

4.4.1   Test results

The Box-Behnken central combination test consisted of 17 groups, including 12 groups of analysis factors and 5 groups of zero-point estimation error tests. The 12 groups of analysis factor tests were repeated 3 times in each group, and the mean value was taken as the final results. The experimental design and results of this study are listed in Table 3. According to the test results, the film collection rate of the residual film recovery machine was 47.57%-69.87%.

Table 3   Test design and results

No.	Factors and levels			Index	No.	Factors and levels			Index
	x_1/mm	x_2/km·h^{-1}	x_3/r·min^{-1}	Y_1/%		x_1/mm	x_2/km·h^{-1}	x_3/r·min^{-1}	Y_1/%
1	60	4	50	48.53	10	100	6	35	59.72
2	140	4	50	58.79	11	100	4	65	60.98
3	60	6	50	47.57	12	100	6	65	51.73
4	140	6	50	51.49	13	100	5	50	68.14
5	60	5	35	49.61	14	100	5	50	68.66
6	140	5	35	55.62	15	100	5	50	69.61
7	60	5	65	47.29	16	100	5	50	68.83
8	140	5	65	56.25	17	100	5	50	69.87
9	100	4	35	58.43	/	/	/	/	/

Note: x_1 is the working depth, mm; x_2 is the forward speed of machinery, km/h; x_3 is the rotation speed of nail-tooth roller, r/min; Y_1 is the residual film collection rate, %.

4.4.2   Regression analysis and significance test

The design-Expert V8.0.6.1 software was used for variance analysis of the test results in Table 4, and the results are listed in Table 5.

According to the results of regression analysis of variance of the test results in Table 4, it can be seen that the p-values of the single factor items x_1, x_2, and x_3, the interaction items x_1x_2 and x_2x_3 were all <0.05, which were highly significant factors for the film collection rate Y_1. The p-value of interaction term x_1x_3 was 0.0873,

which was in the range of 0.05-0.1 and was a significant influencing factor of Y_1. Therefore, the order of the extremely significant factors that affect the film collection rate Y_1 was as follows: $x_1>x_2>x_2x_3>x_1x_2>x_3>x_1x_3$.

Besides, according to the regression variance analysis, the obtained model coefficient of the test result was $p<1×10^{-4}$, the determination coefficient R^2=99.65%, the corrected determination coefficient R^2_{adj}=99.19%, the predicted determination coefficient R^2_{pred}=97.01%, and the coefficient of variation C.V=1.27%. It indicated that the regression model was extremely significant and could be used to analyze and predict the film collection rate Y_1. Then, a second-order response model obtained according to the regression variance analysis result and coding factors is shown in Equation (18):

$$Y = -264.58 + 1.66x_1 + 70.24x_2 + 3.08x_3 - 0.04x_1x_2 + 0.001x_1x_3 - 0.18x_2x_3 - 0.007x_1^2 - 5.95x_2^2 - 0.02x_3^2 \tag{18}$$

Table 4   Regression model variance analysis

Experimental index	Difference source	Sum of squares	Degree of freedom	Mean square	F-value	p-value
	Model	1090.66	9	121.18	219.89	<0.0001
	x_1	106.22	1	106.22	192.73	<0.0001
	x_2	32.89	1	32.89	59.67	0.0001
	x_3	6.35	1	6.35	11.53	0.0115
Residual film collection rate/%	x_1x_2	10.05	1	10.05	18.23	0.0037
	x_1x_3	2.18	1	2.18	3.95	0.0873
	x_2x_3	27.77	1	27.77	50.39	0.0002
	x_1^2	554.40	1	554.40	1005.97	<0.0001
	x_2^2	149.18	1	149.18	270.68	<0.0001
	x_3^2	120.73	1	120.73	219.07	<0.0001
	Residual	3.86	7	0.55		
	Lake of fit	1.85	3	0.62	1.22	0.4097
	Pure error	2.01	4	0.50		

R^2=99.65%, R^2_{adj}=99.19%, R^2_{pred}=97.01%, C.V=1.27%

Note: $p<0.05$ (highly significant); $0.05<p<0.1$ (significant); $p>0.1$(not significant)

Table 5   Test result

Items	Y_1/%			Y_2/%
	Optimal value	Test results	Relative errors	Test results
Value	69.20	66.84	3.40	1.39

4.4.3   Influence analysis of interaction factors

According to the regression model analysis, the interaction terms x_1x_2 and x_2x_3 have a highly significant impact on the test response value Y_1, while the interaction terms x_1x_3 have a significant impact on the test response value Y_1. The influence of each interaction factor on the response value Y_1 as shown in Figure 12.
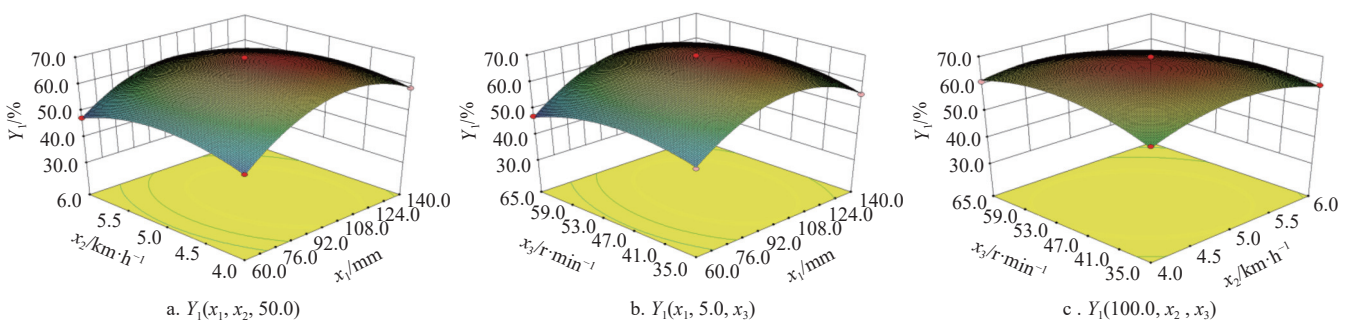
Figure 12   Effects of interaction factors on the residual film collection rate

Figure 12a shows the influence of the interaction between the working depth x_1 and the forward speed of the machine x_2 on the film collection rate Y_1 when the rotation speed of the nail tooth roller x_3 was at 0 levels (x_3=50.0 r/min). When the working depth x_1 increases, the film collection rate Y_1 first increases and then decreases, and the change range was rapid increase. When the forward speed of the machine x_2 increases, the film collection rate Y_1 increases first and then decreases accordingly, but the change amplitude was slower. It means that the influence of the working depth x_1 on the film collection rate Y_1 was more significant than that of the forward speed of the machine x_2 at the test level, which was consistent with the results of the regression model analysis of variance.

Figure 12b shows the influence of the interaction between the working depth x_1 and the rotation speed of the nail tooth roller x_3 on the film collection rate Y_1 when the forward speed of the machine x_2 was at 0 levels (x_2=5.0 km/h). When the working depth x_1 increases, the film collection rate Y_1 first increases and then decreases, and the change range was a rapid increase. When the rotation speed of the nail tooth roller x_3 increases, the film collection rate Y_1 also increases first and then decreases accordingly, but the change amplitude was slower. It means that the influence of the working depth x_1 on the film collection rate Y_1 was more significant than that of the rotation speed of the nail tooth roller x_3 at the test level, which was consistent with the results of the regression model analysis of variance.

Figure 12c shows the influence of the interaction between the forward speed of the machine x_2 and the rotation speed of the nail tooth roller x_3 on the film collection rate Y_1 when the working depth x_1 was at 0 levels (x_1=100.0 mm). It is shown when the forward speed of the machine x_2 increases, the film collection rate Y_1 first increases and then decreases; when the rotation speed of the nail tooth roller x_3 increases, the film collection rate Y_1 also increases gradually. It means that the influence of the forward speed of the machine x_2 on the film collection rate Y_1 was more significant than that of the rotation speed of the nail tooth roller x_3 at the test level, which was consistent with the results of the regression model analysis of variance.

4.5 Optimization and verification

To get the optimal parameters combination of the machine, the optimization module of Design-Expert V8.0.6.1 software was used to optimize working parameters. The constraint conditions of test factors and test indexes were

$$\begin{cases} Y_{\max} = F(x_1, x_2, x_3) \\ \text{s.t} \begin{cases} x_1 \in [80.0, 100.0] \\ x_2 \in [4.5, 5.5] \\ x_3 \in [35.0, 50.0] \end{cases} \end{cases} \quad (19)$$

The results showed that the combination with the highest satisfaction degree was selected as the optimal combination of parameters: the working depth x_1 was 100.0 mm, the forward speed of the machine x_2 was 4.8 km/h, the rotation speed of the nail tooth roller x_3 was 49.3 r/min, and the predicted value of film collection rate Y_1 was 69.2%.

To verify the reliability of the optimization results, the field tests were carried out with the optimal parameter combination. All of the above tests were repeated 5 times, and the results were calculated as an arithmetic average, as listed in Table 5.

The test results show that the average film collection rate of the sowing residual film recovery machine was 66.84%, the film

intertwining rate was 1.39%, and the relative error between the test value and the optimized value of the film collection rate was 3.4%. In addition, the residual film collection rate of the residual film recovery machine is lower than the recovery rate (≥70%) stipulated in the national standard GB/T 25412-2010. The reason is that the quality of the residual film is too small, and the partially recovered residual film appears "flying upside down" under the action of the flow field generated by the film dripping unit, causing the picked up residual film to fly out of the film collection unit, resulting in a decrease in the film collection rate. This issue is also the focus of our follow-up optimization research on film stripping devices.

5 Conclusions

1) An arc-shaped nail-tooth roller plow layer residual film recovery machine was developed based on a radial plate arc-shaped nail-tooth roller structure. The critical parts of the device were designed, and the structural sizes and relevant working parameters were determined.

2) Through the single factor tests, the influence rule of the experimental factors on the experimental index was obtained, and the value range of each influence factor was determined. Through the Box-Behnken response surface test, the order of the extremely significant factors that affect the film collection rate Y_1 were as follows: $x_1 > x_2 > x_2x_3 > x_1x_2 > x_3 > x_1x_3$. And the optimal operating parameters of the residual film recovery machine were determined as follows: the working depth x_1 was 100.0 mm, the forward speed of the machine x_2 was 4.8 km/h, the rotation speed of the nail tooth roller x_3 was 49.3 r/min, and the predicted value of the film collection rate Y_1 was 69.2%.

3) Field test under optimal parameters combination showed that the residual film collection rate was 66.84%, the film intertwining rate was 1.39%, and the relative error between the test value and the optimized value of the film collection rate was 3.4%. It indicates that the machine can accomplish the collection of sowing layer residual film.

Acknowledgements

[References]

[1]   Li P H, Wu B, Gao Y H, Niu J Y, Chen Y J, Ling P, et al. Effect of plastic film mulching on economic benefit of oil flax in dryland-comprehensive evaluation based on entropy weight and grey correlation coupling. Journal of Arid Land Resources and Environment, 2021; 35(4): 180–188. (in Chinese)

[2]   Zhang B C, Chen X G, Liang R Q, Li J L, Wang X Z, Meng H W, et al. Cotton stalk restitution coefficient determination tests based on the binocular high-speed camera technology. Int J Agric & Biol Eng, 2022; 15(4): 181–189.

[3]   Liang R Q, Zhang B C, Chen X G, Meng H W, Wang X Z, Shen C J, et al. Design and test of a multi-edge toothed cutting device for membrane-impurity mixed material. Int J Agric & Biol Eng, 2023; 16(2): 73–84.

[4]   Niu W Q, Zou X Y, Liu J J, Zhang M Z, Li W, Gu J. Effects of residual plastic film mixed in soil on water infiltration, evaporation and its uncertainty analysis. Transactions of the CSAE, 2016; 32(14): 110–119. (in Chinese)

[5]   Zhang Z Y, Li J B, Wang X F, Zhao Y M, Xue S K, Su Z P, et al. Design

and test of 1SMB-3600A type fragmented mulch film collector for sowing layer soil. Soil & Tillage Research, 2022; 225: 105555.

[6] Zhang H M, Chen X G, Yan L M, Yang S M. Design and test of master-slave straw returning and residual film recycling combine machine. Transactions of the CSAE, 2019; 35(19): 11–19. (in Chinese)

[7] Zhang Z Y, Li J B, Wang X F, Zhao Y M, Xue S K, Su Z P. Parameters Optimization and Test of an Arc-Shaped Nail-Tooth Roller-Type Recovery Machine for Sowing Layer Residual Film. Agriculture, 2022; 12(5): 660.

[8] Liang R Q, Chen X G, Jiang P, Zhang B C, Meng H W, Peng X B, et al. Calibration of the simulation parameters of the particulate materials in film mixed materials. Int J Agri & Biol Eng, 2020; 13(4): 29–36.

[9] Zhao Y, Chen X G, Wen H J, Zheng X, Niu Q, Kang J M. Research status and prospect of control technology for residual plastic film pollution in farmland. Transactions of the CSAE, 2017; 48(6): 1–14. (in Chinese)

[10] Liang R Q, Chen X G, Zhang B C, Meng H W, Jiang P, Peng X B, et al. Problems and countermeasures of recycling methods and resource reuse of residual film in cotton fields of Xinjiang. Transactions of the CSAE, 2019; 35(16): 1–13. (in Chinese)

[11] You J H, Zhang B H, Wen H J, Kang J M, Song Y Q, Chen X G. Design and test optimization on spade and tine combined residual plastic film device. Transactions of the CSAM, 2017; 48(11): 1–9. (in Chinese)

[12] Lu B, Wang X F, Hu C, Zhang P F. Design and finite element analysis of cuddle plastic film tooth for plastic film residue collector used on vertical cotton stem. Journal of Agricultural Mechanization Research, 2017; 39(10): 63–66, 71. (in Chinese)

[13] Shi L L, Hu Z C, Gu F W, Wu F, Chen Y Q. Design on automatic unloading mechanism for teeth type residue plastic film collector. Transactions of the CSAE, 2017; 33(18): 11–18. (in Chinese)

[14] Wang K J, Hu B, Luo X, Chen X G, Zheng X, Yan L M, et al. Design and experiment of monomer profiling raking-film mechanism of residue plastic film collector. Transactions of the CSAE, 2017; 33(8): 12–20. (in Chinese)

[15] Ma S H, Zhang X J. Development on 1QZ-3900 Plastic Film Collector. Journal of Agricultural Mechanization Research, 2011; 33(7): 93–96. (in Chinese)

[16] Yan W, Hu Z C, Wu N, Xu H B, You Z Y, Zhou X X. Parameter optimization and experiment for plastic film transport mechanism of shovel screen type plastic film residue collector. Transactions of the CSAE, 2017; 33(1): 17–24. (in Chinese)

[17] Luo K, Yuan P P, Jin W, Yan J S, Bai S H, Zhang C H, et al. Design of chain-sieve type residual film recovery machine in plough layer and optimization of its working parameters. Transactions of the CSAE, 2018; 34(19): 19–27. (in Chinese)

[18] Sun Y, Jian J M, Tian Y T, Sun F C, Zhang M J, Wang S G. Analysis and Experiment of Filming Mechanism of Rotary Film-lifting Device of Residual Film Recycling Machine. Transactions of the CSAM, 2018; 49(S1): 304–310. (in Chinese)

[19] Zhang X J, Liu J Q, Shi Z L, Jin W, Yan J S, Yu M J. Design and parameter optimization of reverse membrane and soil separation device for residual film recovery machine. Transactions of the CSAE, 2019; 35(4): 46–55. (in Chinese)

[20] Xie J H, Yang Y X, Cao S L, Zhang Y, Zhou Y B, Ma W B. Design and experiments of rake type surface residual film recycling machine with guide chain. Transactions of the CSAE, 2020; 36(22): 76–86. (in Chinese)

[21] Liu X F, Shi X, Guo Z F, Wang C Y, Wang X N. Performance test on roller type residual film recycling machine. Transactions of the CSAE, 2017; 33(16): 26–31. (in Chinese)

[22] Xie J H, Zhang F X, Chen X G, Han Y J, Tang W. Design and parameter optimization of arc tooth and rolling bundle type plastic film residue collector. Transactions of the CSAE, 2019; 35(11): 26–37. (in Chinese)

[23] Chen X H, Chen X G, Li J B, Li C S, Yang Y K. Design and test of nail-teeth roller-type residual film recovery device before sowing. Transactions of the CSAE, 2020; 36(2): 30–39. (in Chinese)

[24] Shi Z L, Tang X P, Zhen J, Yan J S, Zhang X J, Jin W. Performance test and motion simulation analysis of nail tooth type mechanism for collecting plastic residue. Transactions of the CSAE, 2019; 35(4): 64–71. (in Chinese)

[25] Hu C, Wang X F, Chen X G, Tang X Y, Zhao Y, Yan C R. Current situation and control strategies of residual film pollution in Xinjiang. Transactions of the CSAE, 2019; 35(24): 223–234. (in Chinese)

[26] He H J, Wang Z H, Guo L, Zheng X R, Zhang J Z, Li W H, et al. Distribution characteristics of residual film over a cotton field under long-term film mulching and drip irrigation in an oasis agroecosystem. Soil & Tillage Research, 2018; 180: 194–203.